

# UNDERSTANDING THE RATIONAL FUNCTION MODEL: METHODS AND APPLICATIONS

Yong Hu, Vincent Tao, Arie Croitoru

GeoICT Lab, York University, 4700 Keele Street, Toronto M3J 1P3 - {yhu, tao, ariec}@yorku.ca

**KEY WORDS:** Photogrammetry, Remote Sensing, Sensor Model, High-resolution, Satellite Imagery

## ABSTRACT:

The physical and generalized sensor models are two widely used imaging geometry models in the photogrammetry and remote sensing. Utilizing the rational function model (RFM) to replace physical sensor models in photogrammetric mapping is becoming a standard way for economical and fast mapping from high-resolution images. The RFM is accepted for imagery exploitation since high accuracies have been achieved in all stages of the photogrammetric process just as performed by rigorous sensor models. Thus it is likely to become a passkey in complex sensor modeling. Nowadays, commercial off-the-shelf (COTS) digital photogrammetric workstations have incorporated the RFM and related techniques. Following the increasing number of RFM related publications in recent years, this paper reviews the methods and key applications reported mainly over the past five years, and summarizes the essential progresses and address the future research directions in this field. These methods include the RFM solution, the terrain-independent and terrain-dependent computational scenarios, the direct and indirect RFM refinement methods, the photogrammetric exploitation techniques, and photogrammetric interoperability for cross sensor/platform imagery integration. Finally, several open questions regarding some aspects worth of further study are addressed.

## 1. INTRODUCTION

A sensor model describes the geometric relationship between the object space and the image space, or vice versa. It relates 3-D object coordinates to 2-D image coordinates. The two broadly used imaging geometry models include the physical sensor model and the generalized sensor model. The physical sensor model is used to represent the physical imaging process, making use of information on the sensor's position and orientation. Classic physical sensors employed in photogrammetric missions are commonly modeled through the collinearity condition and the corresponding equations. By contrast, a generalized sensor model does not include sensor position and orientation information. Described in the specification of the OGC (1999a), there are three main replacement sensor models, namely, the grid interpolation model, the RFM and the universal real-time sensor model (USM). These models are generic, i.e., their model parameters do not carry physical meanings of the imaging process. Use of the RFM to approximate the physical sensor models has been in practice for over a decade due to its capability of maintaining the full accuracy of different physical sensor models, its unique characteristic of sensor independence, and real-time calculation. The physical sensor model and the RFM have their own advantages and disadvantages for different mapping conditions. To be able to replace the physical sensor models for photogrammetric processing, the unknown parameters of the RFM are usually determined using the physical sensor models. The USM attempts to divide an image scene into more sections and fit a RFM for each section. Nevertheless, it appears that one RFM is usually sufficient for modeling a whole image scene with 27552 rows and 27424 columns for a QuickBird PAN image.

The RFM was initially used in the U.S. military community. Gradually, the RFM scheme is becoming well known to the mapping community, largely due to its wide adoption as a new standard. OGC has already decided (1999a) to adopt it as a part of the standard image transfer format. The decision of

commercial companies, such as Space Imaging (the first high-resolution satellite imagery vendor), to adopt the RFM scheme in order to deliver the imaging geometry model has also contributed to the wide adoption of the RFM. Consequently, instead of delivering the interior and exterior orientation geometry of the Ikonos sensor and other physical parameters associated with the imaging process, the RFM is used as a sensor model for photogrammetric exploitation. The RFM supplied is determined by a terrain-independent approach, and was found to approximate the physical Ikonos sensor model very well. Generally, there are two different ways to determine the physical Ikonos sensor model, depending on the availability and usage of GCPs. Without using GCPs, the orientation parameters are derived from the satellite ephemeris and attitude. The satellite ephemeris is determined using on-board GPS receivers and sophisticated ground processing of the GPS data. The satellite attitude is determined by optimally combining star tracker data with measurements taken by the on-board gyros. With GCPs used, the modeling accuracy can be significantly improved (Grodecki and Dial, 2001). Digital Globe (USA) also delivers the RFM for its imagery products with up to 0.6-m resolution, in addition to the spacecraft parameters (e.g., telemetry including refined ephemeris and attitude) and (interior and exterior) orientations of the QuickBird sensor.

Recently, a number of recently published papers have reported the algorithms and methods in the use of RFM for photogrammetric processing on images acquired by different satellite and airborne imaging sensors. Most work have focused on processing the Ikonos *Geo* imagery (up to 1-m resolution) supplied by Space Imaging. The facility of using the RFM to replace physical sensor models in photogrammetric mapping is being incorporated into many COTS software packages, and is becoming a standard way for economical and fast mapping from remotely sensed images. To follow this trend, other imagery vendors possessing medium and high-resolution satellite sensors, such as ORBVUE-3 (ORBIMAGE, USA), RADARSAT (Canada), IRS (India), and SPOT 5 (France), may

also supply RFM-enabled imagery products in the near future.

This paper reviews the developments in the use of the RFM mainly over the past five years to summarize the essential progresses in this field. The methodology of developing the RFM is summarized in Figure 1, where the individual processes and their interrelations are explained in following sections.

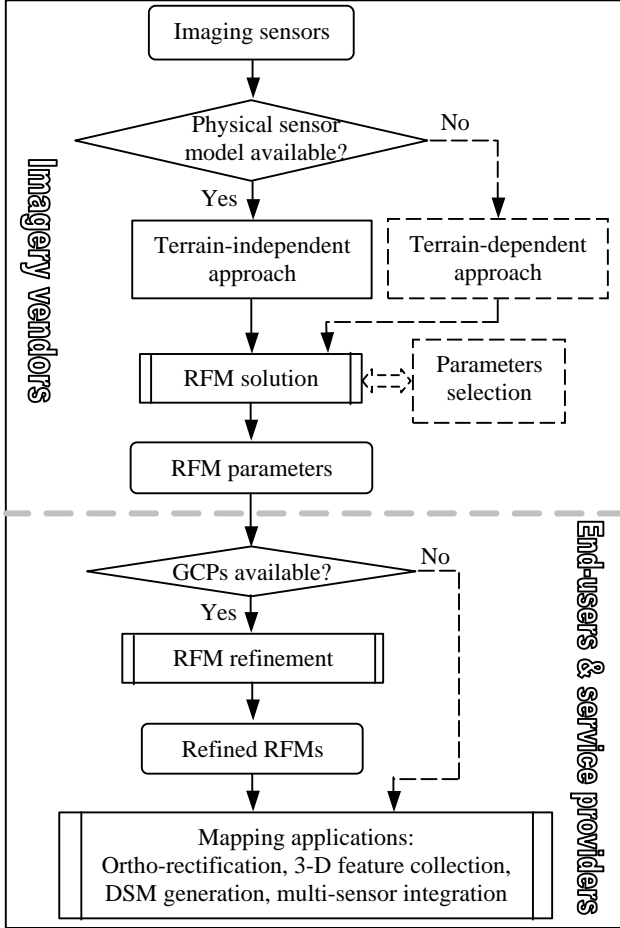


Figure 1. The strategy of developing the RFM

### 1.1 The Rational Function Model

The RFM relates object point coordinates ( $X, Y, Z$ ) to image pixel coordinates ( $l, s$ ) or vice visa, as physical sensor models, but in the form of rational functions that are ratios of polynomials. The RFM is essentially a generic form of the rigorous collinearity equations and the generalized sensor models including the 2-D and 3-D polynomial models, the projective transformation model and the (extended) direct linear transformation model. For the ground-to-image transformation, the defined ratios have the forward form (OGC, 1999a):

$$\begin{aligned} l_n &= p_1(X_n, Y_n, Z_n) / p_2(X_n, Y_n, Z_n) \\ s_n &= p_3(X_n, Y_n, Z_n) / p_4(X_n, Y_n, Z_n) \end{aligned} \quad (1)$$

where ( $l_n, s_n$ ) are the normalized line (row) and sample (column) index of pixels in image space; ( $X_n, Y_n, Z_n$ ) are normalized coordinate values of object points in ground space; polynomial coefficients  $a_{ijk}, b_{ijk}, c_{ijk}, d_{ijk}$  are called rational function coefficients (RFCs). The normalization (i.e., offset and scale) minimizes the introduction of errors during computation (NIMA, 2000). The total power of all ground coordinates is usually limited to three. In such a case, each numerator or

denominator is of twenty-term cubic form, and the order defined in NIMA (2000) has become the de facto industry standard.

The polynomial coefficients are also called RPCs, namely, rapid positioning capability, rational polynomial coefficients or rational polynomial camera data. In this paper, we refer the RFM as general rational functions with some variations, such as subsets of polynomial coefficients, equal or unequal denominators and two transformation directions (i.e., forward and inverse equations). Nine configurations of the RFM have been analyzed in Tao and Hu (2001a, 2001b). An inverse form of the RFM is described in Yang (2000), but is seldom used. The term - RPC model - often refers to a specific case of the RFM that is in forward form, has third-order polynomials, and is usually solved by the terrain-independent scenario. The RPC model is more concentrated because it is transferred with Space Imaging and Digital Globe imagery products.

### 1.2 RFM Solution

The unknown RFCs can be solved by least-squares adjustment. The normal equation is given by Eq. 2 (Tao and Hu, 2001a), where  $I$  is the vector of RFCs;  $T$  is the design matrix of the linearized observation equations (Eq. 1);  $W$  is the weight matrix for image pixel coordinates  $G$ . The covariance matrix associated with  $I$  is given by Eq. 3 (Hu and Tao, 2002), where  $R$  is the covariance associated with the measured image positions.

$$T^T W T I - T^T W G = 0 \quad (2)$$

$$P = (T^T W T)^{-1} + R \quad (3)$$

To tackle the possible ill-conditioning problem during the adjustment, the Tikhonov regularization technique was suggested to turn the normal equation into a regularized one. Then the RFCs may be solved iteratively as follows:

$$I_k = I_{k-1} + (T^T W_{k-1} T + h^2 E)^{-1} T^T W_{k-1} w_{k-1} \text{ for } k = 1, 2, \dots \quad (4)$$

with  $I_0 = 0, W_0 = W(I_0) = E$

where  $h$  is the regularization parameter;  $k$  is the iteration number;  $W_k = W(I_k)$  is the weight matrix;  $w_k = G - T I_k$  is the misclosures at GCPs.

## 2. APPROACHES OF DETERMINING RFCS

The RFCs can be solved by terrain-independent scenario using known physical sensor models or by terrain-dependent scenario without using physical sensor models.

### 2.1 Terrain-independent Approach

For the terrain-independent scenario, the RFM performs as a fitting function between the image grid and the object grid (Yang, 2000; Tao and Hu, 2001a). In detail, an image grid covering the full extent of the image is established and its corresponding 3-D object grid with several layers (e.g., four or more layers for the third-order case) slicing the entire elevation range is generated. The horizontal coordinates ( $X, Y$ ) of a point of the 3-D object grid are calculated from a point ( $l, s$ ) of the image grid using the physical sensor model with specified elevation  $Z$ . Then the RFCs are estimated using a direct least-squares solution with an input of the object grid points and the image grid points. The regularization technique is not needed because the linearized observation equations are well conditioned. However, the regularization may help produce well-structured RFCs, among which the 2<sup>nd</sup> and 3<sup>rd</sup>-order coefficients will be constrained to be close to 0, and the constant and 1<sup>st</sup>-order components represent the optical

projection more closely (Hartley and Saxena, 1997). This would also be useful in estimating the approximate object coordinates using only the low-order terms in 3-D reconstruction. The RFM determined this way is proved to be able to achieve a very high approximating accuracy to original physical sensor models. It is reported that the RPC model yields a worst-case error below 0.04 pixel for Ikonos imagery compared with its rigorous sensor model under all possible acquisition conditions (Grodecki and Dial, 2001). Therefore, when the RFM is used for imagery exploitation, the achievable accuracy is virtually equivalent to the accuracy of the original physical sensor model. This terrain-independent computational scenario makes the RFM a perfect and safe replacement to the physical sensor models, and has been widely used to determine the RFCs.

## 2.2 Terrain-dependent Approach

For the terrain-dependent scenario, the RFM tries to approximate the complicated imaging geometry across the image scene using its plentiful polynomial terms without establishing the grids, and the solution is highly dependent on the actual terrain relief, the distribution and the number of GCPs. GCPs on the 2.5-D terrain surface have to be collected by the conventional ways (e.g. measured on topographical maps or by GPS, and on aerial or satellite imagery). The iterative least-squares solution with regularization is then used to solve for the RFCs. In this context, the RFM behaves as a rubber-sheeting model, and the over-parameterisation may cause the design matrix of the normal equations to become almost rank deficient because of the complex correlations among RFCs. The regularization technique improves the condition of the design matrix, and thus avoids numerical instability in the least-squares adjustment. There are also many experiments carried on using frame, pushbroom or SAR images to assess the approximating ability of the RFM obtained in this manner, and the accuracy is high provided that a large number (for instance, as twice as the minimum number of GCPs required to obtain a close-form solution) of evenly distributed GCPs are collected across the whole scene. Nevertheless, the terrain-dependent approach may not provide a sufficiently accurate and robust solution if the above requirements for control information are not satisfied. Therefore, the RFM solved by terrain-dependent approach may not be used as a replacement sensor model if high accuracy is required (Toutin and Cheng, 2000; Tao and Hu, 2001a, b).

## 3. RFM REFINING METHODS

As proved by its high approximating accuracy to many physical sensor models, the RFM has high capability of geometric interpolation. However, the RPCs provided by imagery vendors may not always approximate the real imaging process well. The requirements for control information may be not met satisfactorily sometimes, or no ground control information is used when determining the physical sensor model itself for different marketing strategies from imagery vendors. High precision products are sold at a significantly higher price, and even require that users provide GCPs and a DTM. This presents a problem for many users who are prohibited to release topographic data this way.

Recent studies have found that RPCs can be refined in the domain of the image space or of the ground space, when additional control information becomes available. For example, the Ikonos *Geo* products and *Standard* stereo products will be improved to sub-meter absolute positioning accuracy using one

or more high quality GCPs (Grodecki and Dial, 2003; Fraser et al, 2003; Tao and Hu, 2004) or be close to the accuracy of the GCPs whose quality is low (Hu and Tao, 2002; Tao et al. 2003). So the RFM refining methods will definitely promote the use of low pricing products for many applications.

The RFM may be refined directly or indirectly. The direct refining methods update the original RPCs themselves. So the updated RPCs can be transferred without the need for changing the existing image transfer format. While the indirect refining introduces complementary or concatenated transformations in image or object space, and they do not change the original RPCs directly. The affine transformation or a translation for the simplest case is often used. In addition, tie points can be measured on multiple images, and their models may be refined resulting better relative orientation after block adjustment. In essence, the two-step procedure of the in-direct refinement can be combined into one by recalculate the RPCs with a pair of 3-D object grid and 2-D image grid established for each image.

### 3.1 Direct Refining Methods

The RPCs can be recomputed using the batch method (called RPC-BU) when both the original and the additional GCPs are available (Hu and Tao, 2002; Di et al., 2003). Here, the original GCPs refer to those used to compute the existing RPCs, whereas the additional GCPs are independently collected and are not used to solve the initial RPC values. The refinement is fulfilled by incorporating all of the GCPs into the RPCs solution, with both the original and new GCPs appropriately weighted. The values of the existing RPCs may be used as the initial solution  $I_0$  to speedup the convergence in Eq. 4. While only the new GCPs are available, the existing RPCs can be updated using an incremental method (called RPC-IU) based on the Kalman filtering or sequential least-squares (Hu and Tao, 2002; Bang et al., 2003). That is, the RPCs are corrected by adding weighted residuals from the new measurements. The corrections of the approximate RPCs  $I_k$  are given by

$$\Delta I_k = P_k^{-1} T_k^T (T_k P_k^{-1} T_k^T + R_k)^{-1} \cdot (G_k - T_k I_k) \text{ for } k = 1, 2, \dots \quad (5)$$

where  $P_k^{-1}$  is the covariance matrix associated with  $I_k$ ;  $T_k$  is the design matrix made from new GCPs;  $R_k$  is the covariance matrix associated with the image pixel coordinates  $G_k$  of new GCPs. The error propagations on both the RPCs and the new GCPs are recorded during the updating process. Satisfactory accuracy improvements can be expected in both image domain and object domain when the covariance matrix  $P_k^{-1}$  is known.

### 3.2 In-direct Refining Methods

When the RPCs are fit to a physical sensor model whose orientation parameters are derived from satellite ephemeris and attitude information without requiring the use of GCPs, mainly linear systematic errors exist. To refine the forward RFM, it is more suitable by appending a simple complementary transformation in image space at the right side of Eq. 1 to eliminate the error sources. For narrow field-of-view CCD instruments with a priori orientation data, these physical effects mainly behave like a same net effect of displacements in line and sample directions in image plane in total. Fraser and Hanley (2003) used two bias parameters to compensate the lateral shift of the sensor platform in two orthogonal directions under the assumption that the biases manifest themselves for all practical purposes as image coordinate perturbations. Grodecki and Dial (2003) proposed a comprehensive block adjustment math model (called RPC-BA). The formulation uses two complementary

polynomials that are adjustable to model the effects originated from the uncertainty of spacecraft telemetry and geometric properties of the Ikonos sensor. The first-order polynomials  $\Delta l$  and  $\Delta s$  are defined by

$$\begin{aligned}\Delta l &= l' - l = a_0 + a_l \cdot l + a_s \cdot s \\ \Delta s &= s' - s = b_0 + b_l \cdot l + b_s \cdot s\end{aligned}\quad (6)$$

where  $(\Delta l, \Delta s)$  express the discrepancies between the measured line and sample coordinates  $(l', s')$  and the RFM projected coordinates  $(l, s)$  of a GCP or tie point; the coefficients  $a_0, a_l, a_s, b_0, b_l, b_s$  are the adjustment parameters for each image. Grodecki and Dial (2003) indicated that each of the polynomial coefficients has physical significance for Ikonos products, and thus the RPC-BA model does not present the numerical instability problem. In detail, the constant  $a_0$  ( $b_0$ ) absorbs all in-track (cross-track) errors causing offsets in the line (sample) direction, including in-track (along-track) ephemeris error, satellite pitch (roll) attitude error, and the line (sample) component of principal point and detector position errors. Because the line direction is equivalent to time, parameters  $a_l$  and  $b_l$  absorb the small effects due to gyro drift during the imaging scan. Tests show that the gyro drift during imaging scan turn out to be neglectable for image strips shorter than 50 km. Parameters  $a_s$  and  $b_s$  absorb radial ephemeris error, and interior orientation errors such as focal length and lens distortion errors. These errors are also negligible for Ikonos. Thus, for an Ikonos image shorter than 50 km, the adjustment model becomes simply  $\Delta l = a_0$  and  $\Delta s = b_0$ , where  $a_0$  and  $b_0$  are bias parameters used in Fraser and Hanley (2003). The correction vector to the approximate values of both the model parameters and the object point coordinates is given by Eq. 7 (Grodecki and Dial, 2003), where  $A$  is the design matrix of the block adjustment equations;  $w$  is the vector of misclosures for model parameters;  $C_w$  is the covariance matrix.

$$\Delta x = (A^T C_w^{-1} A)^{-1} A^T C_w^{-1} w \quad (7)$$

The concatenated transformations also introduce additional parameters (e.g., of polynomials) in either image space or object space. They try to improve the positioning accuracy by fitting the RFM calculated coordinates to the measured coordinates of new GCPs. Thus, the ground-to-image transformation becomes a concatenated transformation with the original forward RFM transform as the first step and the additional transform (e.g., polynomials) as the second step. Because the forward RFM is more used in industry, it is straightforward to apply an additional transformation in image space. The 2-D affine transformation in image space (called RPC-CT), i.e.,

$$\begin{aligned}l' &= a_0 + a_1 \cdot l + a_2 \cdot s \\ s' &= b_0 + b_1 \cdot l + b_2 \cdot s\end{aligned}\quad (8)$$

are tested in Bang et al. (2003) and Tao et al. (2004). It is observed that the values of  $a_1$  and  $b_2$  are always close to 1, and  $a_2, b_1$  close to 0 when refining the Ikonos and QuickBird images. Di et al. (2003) used polynomials in ground space. The known RFMs of two or more images are employed to intersect the ground coordinates of object points from their measured conjugate image points. Then the intersected ground coordinates are fit to the measured ground coordinates of GCPs to solve for the coefficients of the polynomials.

#### 4. PHOTOGRAMMETRIC EXPLOITATION

Orthorectification and stereo intersection are two most important methods for preparing fundamental data for

cartographic mapping applications. The RFM can be used to perform the photogrammetric processing on images since it is a generic form of many imagery geometry models and has inherent geometric modeling capability.

An original un-rectified aerial or satellite image does not show features in their correct locations due to displacements caused by the tilt of the sensor and the relief of the terrain. Orthorectification transforms the central projection of the image into an orthogonal view of the ground with uniform scale, thereby removing the distorting affects of tilt optical projection and terrain relief. The RFM based orthorectification is relatively straightforward. The use of RFM for image rectification is discussed in Yang (2000), Dowman and Dolloff (2000), Tao and Hu (2001b), and Croitoru et al. (2004). The orthorectification accuracy is similar to the approximating accuracy of the RFM, excluding the resampling error.

The 3-D reconstruction algorithms can be implemented based on either the forward RFM or the inverse RFM. The approximate values of the un-normalized object point coordinates  $(X, Y, Z)$  are corrected by the correction given by the following formula (Tao and Hu, 2002):

$$(\Delta X \ \Delta Y \ \Delta Z)^T = (A^T W A)^{-1} A^T W l \quad (9)$$

where  $(\Delta X, \Delta Y, \Delta Z)$  are un-normalized coordinate corrections;  $A$  is the design matrix that is composed of ratios between the partial derivatives of the functions in Eq. 1 with respect to  $X, Y$ , and  $Z$  and the image domain scale parameters;  $l$  is the vector of discrepancies between the measured and the RFM projected image coordinates of the estimated object coordinates;  $W$  is the weight matrix for the image points. The weight matrix may be an identity matrix when the points are measured on images of a same sensor type. However, higher weights should be assigned to points measured in images of higher resolution when implementing a hybrid adjustment using images with different ground resolutions as described in the next section. The approximate object coordinates may be obtained by solving the RFM with only constant and first-order terms, or by solving using one image and a given elevation value, or by setting to be the offset values of the ground coordinates. In most cases, eight iterations are enough to converge. A procedure similar to above forward RFM 3-D reconstruction is described in Di et al. (2001), and Fraser and Hanley (2003). But their algorithm does not incorporate the normalization parameters into the adjustment equations directly. The 3-D mapping capability will be greatly enhanced after absorbing one or more GCPs (Fraser et al. 2003; Tao et al., 2004; Croitoru et al., 2004).

#### 5. PHOTOGRAMMETRIC INTEROPERABILITY

Multiple different image geometry models are needed for exploiting different image types under different conditions (OGC, 1999b). There are many different types of imaging geometries, including frame, panoramic, pushbroom, whiskbroom and so on. Many of these imaging geometries have multiple subtypes (e.g. multiple small images acquired simultaneously) and multiple submodels (e.g. atmospheric refraction, panoramic and scan distortions). These image geometries are sufficiently different that somewhat different rigorous image geometry models are required. Furthermore, different cameras of the same basic geometry can require different rigorous image geometry models. When interoperation of several software packages is needed to complete one imagery exploitation service, it is necessary to standardize those

different image geometry models that are expected to have widespread use by interoperable software. OGC (1999b) has adopted a specification for standardization of image geometry models. In photogrammetry, the block adjustment and 3-D mapping often are performed using images acquired by a same sensor and platform. But when the images are acquired by different sensors, the block adjustment among different image geometry models is hard to be implemented due to a combinatorial overflow. Moreover, while many more imaging sensors have been launched or will be launched in near future, it is obviously not convenient for end users and service providers to constantly upgrade their software to process new sensor data. As a matter of fact, the software upgrades often fall behind the availability of the data. This is also expensive and in particular not necessary for many mapping applications requiring accuracy at sub-metre level or lower.

Because of the characteristic of sensor independence, the use of RFM would be a driving force towards the photogrammetric interoperability among imagery exploitation software. If each overlapping image comes with a set of RPCs, end users and developers will be able to perform the subsequent photogrammetric processing neither knowing the original sophisticated physical sensor model nor taking account of the submodels associated with the sensors used to acquire the images. This is highly beneficial as it makes the photogrammetric processing interoperable, thus allowing users and service providers to easily integrate cross sensor/platform images from multiple data vendors. The different image resolution and the error estimates associated with the RPCs for each image should be processed by appropriate weighting during the adjustment. For example, the covariance matrix  $C_w$  in Eq. 7 will use different sub-covariance matrixes of misclosures for the image points measured on different images participating in the adjustment. Thus many of the difficulties that may arise from simultaneously adjusting different physical sensor models can be avoided. This technique is of unique value for users who require high updating rate and for other applications in which high temporal accuracy is of essence.

## 6. PHOTOGRAMMETRIC APPLICATIONS

Many COTS photogrammetric suites have implemented the RFM and related techniques, including ERDAS IMAGINE (LH Systems), PCI Geomatica (PCI), SOCET SET (BAE Systems), ImageStation (Z/I Imaging), and SilverEye (GeoTango). Using these systems, traditional photogrammetric processing tasks can be performed in a unified technical framework. Many mapping applications using above photogrammetric systems or proprietary packages have been reported. We will briefly focus on the photogrammetric applications below.

Kay et al. (2003) evaluated the geometric quality of orthorectifying QuickBird and Ikonos images, for a typical agriculture area, using GCPs and a DTM derived from the 1:50000 scale map data. Two QuickBird images with Basic and Standard levels and an Ikonos Geo image, covering an area of 108 km<sup>2</sup> are rectified. Both results are well with 1:10000 scale accuracy requirements of the EU Common Agriculture Policy.

Fraser et al. (2002) investigated the application of Ikonos imagery to 3-D positioning and building extraction. The results of 2-D and 3-D metric accuracy tests shows a planimetric accuracy of 0.3-0.6 m and height accuracy of 0.5-0.9 m. Tao et al. (2004) evaluated the 3-D feature extraction results using two

Ikonos Reference stereo scenes at a nuclear plant. The relative planimetric and vertical accuracies for 3-D features are at the sub-metre level, and the RFM refinements do not change the relative accuracy.

Tao and Hu (2004) reported 3-D feature extraction results from overlapped QuickBird and Ikonos image pairs. The conjugate points in the QuickBird and the Ikonos images were manually positioned and were assigned different weighting factors of 1 for the Ikonos image and  $1/0.6^2$  for the QuickBird image in Eq. 9. When the RPC models are bias compensated using three GCPs, the object points have the position differences of 1.36-m RMSE horizontally and 0.84-m RMSE vertically, and the dimension differences are better than 1-m RMSE.

## 7. DISCUSSION AND OUTLOOK

Extensive tests have been carried using different formulations of the RFM. These experimental results have revealed that the third-order RFM is not always the best form in terms of obtaining highest approximating accuracy (Tao and Hu, 2001a, 2001b; Fraser et al., 2002). Yang (2000) also reported functions lower than third order were used and the correct order can be chosen, based on the RMS error analysis, testing aerial photography and SPOT data. Hanley and Fraser (2001) tested Ikonos Geo product by first projecting the control points onto 'planes of control', to minimize the effect of terrain, and then transform the image to these points using similarity, affine and projective transformations. The results show that 0.3-0.5 m positioning accuracy is achievable from the *Geo* product without using the rational function solution. Fraser et al. (2002) and Fraser and Yamakawa (2003) have extended this work in two dimensions into three, using similar techniques. They found that the affine projection, the DLT and relief corrected affine transformation also can approximate the Ikonos imaging geometry to sub-metre positioning accuracy in the absence of high-order error sources. If the most significant coefficients could be found for each particular imaging sensor heuristically (e.g., by trial-and-error), then the RFM may be solved with higher stability in the terrain-dependent approach using a small number of GCPs, and may be also suitable for replacing rigorous sensor models as what has been done by terrain-independent approach.

Fraser and Hanley (2004) found the systematic residual errors in the along track direction due to perturbations in scan velocity. The question is then should high order polynomial be used to compensate for this high-order drift error when the errors are not well modeled in the physical sensor model.

Furthermore, currently, Digital Globe also provides images each with multiple sections. Each section is stored in a separate image file using the same set of RPCs with different line and sample offsets. Yet, if each image section has a different set of RPCs as defined in the USM, all the related photogrammetric processing methods have to be re-formulated.

The characteristics of cross sensor imagery exploitation will instigate a crossover of images from multiple data vendors into a new 3-D mapping paradigm. From the viewpoint of imagery exploitation services providers, the RFM technology enables extensive interoperability between images from different sources, regardless of the sensor types and the platforms, due to its geometric generality. However, new problems arise when we try to generate DSMs automatically using heterogeneous images

with different radiometric and scale properties. For example, aerial or satellite images may differ from each other with respect to scale, spectral range of recording, image quality and imaging conditions (weather, lighting). In practice, matching heterogeneous images may prove to be more difficult than implementing the triangulation of different sensor models. Rigorous analysis on the error propagation for cross sensor photogrammetric processing is also of great importance since the imaging geometry and the accuracies may be different among multiple satellites and sensors. However, the difference of fitting accuracy of the RPC models to individual physical sensor models seems neglectable since the accuracy loss is neglectable for the terrain-independent approach.

## 8. CONCLUDING REMARKS

Some high-resolution satellite imagery vendors such as Space Imaging and Digital Globe currently provide the RPCs to end users and service providers to allow for photogrammetric processing. This technology simplifies the complicated photogrammetric mapping process to a great extent, and has been proved to be a useful tool for exploiting high-resolution satellite images. The RFM may be used to replace the rigorous sensor models for many mapping applications because high accuracies have been achieved in exploiting images. And the scepticism on the accuracy achievable has been replaced with a wide the adoption of this technology.

This paper provides an overview of various aspects in developing the RFM, including computational scenarios, accuracy assessment, RFM refinement, photogrammetric interoperability, and mapping applications. Photogrammetrists have overcome restrictions placed on the use of the data by vendors using RFM refining methods, which ensure that the exploitation results are as accurate as what can be achieved using physical sensor models, and are also economical using low price products. The RFM provides an open standard for photogrammetric interoperability, is not dependent on particular sensors, and is extensible for block adjustment. In summary, although there are still remaining issues, the RFM is likely to become a passkey in geometry modeling of various sensors.

## 9. REFERENCES

- Bang, K.I., Jeong, S., Kim, K., 2003. Modification of sensor model parameters with a few GCPs, *ASPRS Annual Conference*, 3-9 May, Anchorage, AK, 6 p.
- Croitoru, A., Hu, Y., Tao, V., Xu, J., Wang, F., Lenson, P., 2004. Single and stereo based 3-D metrology from high-resolution imagery: methodologies and accuracies, *IAPRS*, 12-23 July, Istanbul, 6 p.
- Di, K., Ma, R., Li, R., 2003. Rational functions and potential for rigorous sensor model recovery, *PE&RS*, 69(1), pp. 33-41.
- Dowman, I., Dolloff, J., 2000. An evaluation of rational functions for photogrammetric restitution, *IAPRS*, pp. 254-266.
- Fraser, C., Baltsavias, E., Gruen, A., 2002. Processing of Ikonos imagery for submetre 3D positioning and building extraction, *ISPRS Journal of PRS*, 56, pp. 177-197.
- Fraser, C., Hanley, H., 2003. Bias compensation in rational functions for Ikonos satellite imagery, *PE&RS*, 69, pp. 53-58.
- Fraser, C., Hanley, H., 2004. Bias-compensated RPCs for sensor orientation of high-resolution satellite imagery, *ASPRS Annual Conference*, 23-28 May, Denver.
- Fraser, C., Yamakawa, T., 2003. Applicability of the affine model for Ikonos image orientation over mountainous terrain, *Workshop on HRM from Space*, 6-8 October, Hanover, 6 p.
- Grodecki, J., Dial, G., 2001. Ikonos geometric accuracy, *Joint ISPRS Workshop on HRM from Space*, 19-21 Sept., pp. 77-86.
- Grodecki, J., Dial, G., 2003. Block adjustment of high-resolution satellite images described by rational functions, *PE&RS*, 69(1), pp. 59-69.
- Hanley, H., Fraser, C., 2001. Geopositioning accuracy of Ikonos imagery: indications from 2D transformations. *Photogrammetric Record*, 17(98), pp. 317-329.
- Hartley, R.I., Saxena, T., 1997. The cubic rational polynomial camera model, *DARPA IUW*, pp. 649-653.
- Hu, Y., Tao, V., 2002. Updating solutions of the rational function model using additional control information, *PE&RS*, 68(7), pp. 715-724.
- Kay, S., Sprugt, P., Alexandrou, K., 2003. Geometric quality assessment of orthorectified VHR space image data, *PE&RS*, 69(5), pp. 484-491.
- NIMA, 2000. *The Compendium of Controlled Extensions for the National Imagery Transmission Format (NITF)*. URL: <http://164.214.2.51/ntb/baseline/stdi0002/final.pdf>.
- OpenGIS Consortium (OGC), 1999a. *The OpenGIS Abstract Specification - Topic 7: Earth Imagery*. URL: <http://www.opengis.org/docs/99-107.pdf>.
- OpenGIS Consortium, 1999b. *The OpenGIS Abstract Specification - Topic 16: Image Coordinate Transformation Services*, URL: <http://www.opengis.org/docs/99-116r2.pdf>.
- Tao, V., Hu, Y., 2001a. A comprehensive study on the rational function model for photogrammetric processing, *PE&RS*, 67(12), pp. 1347-1357.
- Tao, V., Hu, Y., 2001b. Use of the rational function model for image rectification. *CJRS*, 27(6), pp. 593-602.
- Tao, V., Hu, Y., 2002. 3-D reconstruction algorithms with the rational function model, *PE&RS*, 68(7), pp. 705-714.
- Tao, V., Hu, Y., 2004. RFM: an open sensor model for cross sensor mapping, *ASPRS Conference*, 23-28 May, Denver, 9 p.
- Tao, V., Hu, Y., Jiang W., 2003. Photogrammetric exploitation of Ikonos imagery for mapping applications, *IJRS*, 25(12).
- Toutin, T., Cheng, P., 2000. Demystification of Ikonos. *Earth Observation Magazine*, 9(7), pp. 17-21.
- Yang, X., 2000. Accuracy of rational function approximation in photogrammetry, *ASPRS Annual Conference*, 22-26 May, 11 p.